arXiv:1404.0759v2 [hep-ph] 9 Dec 2015

A determination of the flavor asymmetric sea quarks in the proton

Wei Zhu[1], Rong Wang[2,3], Jianhong Ruan[1], Xurong Chen[2], Pengming Zhang[2]
[1] *Department of Physics, East China Normal University, Shanghai 200062, China*
[2] *Institute of Modern Physics, Chinese Academy of Sciences, Lanzhou 730000, China*
[3] *Lanzhou University, Lanzhou 730000, China*

Using DGLAP evolution equation with the corrections of parton recombinations, the flavor asymmetric sea quark distributions in the proton are first extracted from the available experimental data with the global QCD analysis method. Comparisons of our predictions to the CTEQ, MRS, and GRV parton distribution functions for sea quarks are presented. Based on the separation of the flavor symmetric and asymmetric sea, the possible relations between strange quark distribution and symmetric light quark distribution are discussed. The results are used to explain the recent HERMES result of the strange quark distribution.

PACS numbers: 12.38.Lg, 14.20.Dh, 11.30.Hv

I. INTRODUCTION

The observation of the violation of Gottfried sum rule [1] from the deep inelastic scattering (DIS) experiment [2, 3], the surprisingly large asymmetry between the up (u) and down (d) antiquark distributions in the proton measured from the Drell-Yan pair production [4, 5] and the semi-inclusive [6] processes revealed a new light on the origins of the nucleon sea. While we still have not an adequate theory for the flavor asymmetry of sea quarks, the flavor asymmetric sea as a new recognized partonic component should be extracted from the experimental data in order to gain deeper and more precise insights of the nucleon structure. Although the sea quark distributions of several widely used parton distribution functions (PDF) [7–9] of the proton are updated using the Dokshitzer-Gribov-Lipatov-Altarelli-Parisi (DGLAP) equation [10–12] to the experimental measurements, the symmetric and asymmetric sea quark components have not been completely separated yet. The solutions of QCD evolution equation depend on the initial parton distributions at an arbitrary low scale $Q_0^2 \sim 1$ GeV^2. The difficulty is that the asymmetric sea always mixes with the symmetric sea since the gluons are already produced at the scale Q_0^2.

The flavor asymmetric sea is created by the nonperturbative QCD process since the perturbative processes cannot cause a significant difference between $\overline{d}$ and $\overline{u}$. One novel way to separate the asymmetric sea from the symmetric sea is to perform the QCD evolution starting from an low enough resolution scale μ^2 where the nucleon contains only the nonperturbative valence and asymmetric sea quarks while the flavor symmetric sea quarks and gluons are not produced at this initial scale. Once the asymmetric sea distributions at μ^2 are determined, they will be given at any $Q^2 > \mu^2$, which can be used to explain the experiments or to make predictions.

It has been known that the application of the standard DGLAP equation is invalid at $Q^2 < 1$ GeV^2 and this equation should be modified at small x and low Q^2 due to the correlations among partons. These nonlinear effects among partons to the DGLAP evolution have been shown in the perturbative QCD [13, 14]. Particularly, the present theory including the complete parton recombinations in the leading order (LO) approximation are derived by Zhu, Ruan and Shen (ZRS) [15–17]. Numerical calculations [18] show that the negative nonlinear corrections can slow down the gluon splitting and improve the perturbative stability of the QCD evolution at low Q^2. Although the contributions of the nonperturbative QCD effects to the measured structure functions at $\mu^2 < Q^2 < 1$ GeV^2 (for example, the hadronic components in the virtual photon) are necessary, these nonperturbative effects are strongly Q^2-power suppressed and they don't participate in the evolution of the parton distributions. It is found that the predicted parton distributions at $Q^2 > 1$ GeV^2 of this approach are consistent with the experiments.

In this work, the asymmetric light sea and the valence quark distributions at the initial scale μ^2 in the proton are determined from the experimental data. With the nonlinear corrections considered, parton distributions are evolved starting from a low resolution scale μ^2, where the nucleon consists entirely of the nonperturbative components. All symmetric sea quarks and gluons are radioactively produced from the QCD fluctuations. The asymmetric sea is completely separated from the symmetric sea.

With the separated symmetric light sea distributions, we speculate some possible relations between the strange quark distribution and the symmetric light quark distribution. These results can be used to check the predictions of various models for the flavor structure of the proton and to improve the current PDFs. The organization of the paper is as follows. Section II presents the analysis method and the ZRS corrections to the DGLAP evolution equation. Comparisons with the experimental data and the predictions of various models are presented in Sec. III. Discussions and a summary are given in Sec. IV. The simplification of the complete nonlinear corrections is presented in the appendix.

II. ANALYSIS METHOD

In this analysis, $q^v(x,Q^2)$ (q=u,d) denote the valence quark distributions, $q^s(x,Q^2)=\overline{q}^s(x,Q^2)$ (q=u,d,s...) denote the symmetric sea quark distributions, $q^{as}(x,Q^2)=\overline{q}^{as}(x,Q^2)$ (q=u,d) denote the asymmetric sea quark distributions, and $g(x,Q^2)$ denotes the gluon distribution. The flavor non-singlet (NS) distribution is defined as $q^{NS}(x,Q^2)=[q^v(x,Q^2)+q^{as}(x,Q^2)+\overline{q}^{as}(x,Q^2)]$, and the flavor-singlet distribution is defined as $\Sigma(x,Q^2)=\sum_q[q^{NS}(x,Q^2)+q^s(x,Q^2)+\overline{q}^s(x,Q^2)]$. We take the parton-antiparton symmetry for the sea quarks and the isospin symmetry for the flavor symmetric sea $\overline{u}^s=\overline{d}^s$. The possible asymmetry for the strange sea $s(x)\neq\overline{s}(x)$ is not considered in this work since it refers to a different mechanism. The present study is focused only on the flavor asymmetric light sea.

The F_2 [19–24], xF_3 [25–27], $\overline{d}-\overline{u}$ and $\overline{d}/\overline{u}$ [4–6] data are used to extract the flavor asymmetric light sea component. The $F_2(x,Q^2)$ data are taken to determine the non-singlet quark distributions $u^{NS}(x,Q^2)$ and $d^{NS}(x,Q^2)$. To separate $u^{as}(x)$ and $d^{as}(x)$ from $u^v(x)$ and $d^v(x)$, we can use the average structure function of the neutrino and antineutrino scattering on the iso-scalar nuclei,

$$xF_3(x,Q^2)=\frac{1}{2}[xF_3^{\nu N}(x,Q^2)+xF_3^{\overline{\nu}N}(x,Q^2)]=xu^v(x,Q^2)+xd^v(x,Q^2). \tag{1}$$

Thus we have

$$\begin{aligned} u^{as}(x,Q^2)+d^{as}(x,Q^2)&=u^{NS}(x,Q^2)+d^{NS}(x,Q^2)-u^v(x,Q^2)-d^v(x,Q^2)\\ &=u^{NS}(x,Q^2)+d^{NS}(x,Q^2)-xF_3(x,Q^2). \end{aligned} \tag{2}$$

On the other hand,

$$d^{as}(x,Q^2)-u^{as}(x,Q^2)=\overline{d}(x,Q^2)-\overline{u}(x,Q^2), \tag{3}$$

are already measured in the E866 [4, 5] and HERMES [6] experiments. In principle, the initial asymmetric light sea distributions can be directly determined combining Eqs. (2) and (3). Unfortunately, the distributions of the asymmetric sea quarks are much smaller than that of the valence quarks. Therefore, the experimental errors of F_2 and xF_3 may hinder us to extract the distributions q^{as}. Instead, the initial parton distributions in this work are parametrized and determined by a global QCD fit to the experimental data of F_2, xF_3, $\overline{d}-\overline{u}$ and $\overline{d}/\overline{u}$.

The parametrization of the initial parton distributions is written as

$$\begin{aligned} xu^v(x,\mu^2)&=Ax^B(1-x)^C(1+D\sqrt{x}+Ex),\\ xd^v(x,\mu^2)&=F(1-x)^G xu^v,\\ x\overline{u}^{as}(x,\mu^2)&=A^{uas}x^{B^{uas}}(1-x)^{C^{uas}}[(1-x)^{D^{uas}}+E^{uas}],\\ x\overline{d}^{as}(x,\mu^2)&=A^{das}x^{B^{das}}(1-x)^{C^{das}}[(1-x)^{D^{das}}+E^{das}]. \end{aligned} \tag{4}$$

At the initial scale μ^2, there are no symmetric sea quarks and gluons, which is written as

$$\begin{aligned} u^s(x,\mu^2)&=\overline{u}^s(x,\mu^2)=0,\\ d^s(x,\mu^2)&=\overline{d}^s(x,\mu^2)=0,\\ s(x,\mu^2)&=\overline{s}(x,\mu^2)=0,\\ g(x,\mu^2)&=0. \end{aligned} \tag{5}$$

Besides, the initial parton distributions are constrained by the two following sum rules, which are expressed in the form

$$\int_0^1 dx x[u^{NS}(x,\mu^2) + d^{NS}(x,\mu^2)] = 1, \tag{6}$$

for the momenta of partons and

$$\begin{aligned} \int_0^1 dx u^{NS}(x,Q^2) &= 2 + 2 < u^{as} >_1, \\ \int_0^1 dx d^{NS}(x,Q^2) &= 1 + 2 < d^{as} >_1, \end{aligned} \tag{7}$$

for the initial numbers of the nonperturbative partons, where $< q >_1$ is the first moment of the distribution q. In the global fit, the value $< d^{as} >_1 - < u^{as} >_1$ is fixed at 0.118 by the experimental measurement [5].

DGLAP equation with ZRS corrections at leading order [15–17] is applied in the work to evolve the nonperturbative initial parton distributions. Here we use the simplified form of the equation for simplicity (see appendix), which is expressed as

$$\begin{aligned} & Q^2 \frac{dxq^{NS}(x,Q^2)}{dQ^2} \\ &= \frac{\alpha_s(Q^2)}{2\pi} P_{qq} \otimes q^{NS}, \end{aligned} \tag{8}$$

for the flavor non-singlet quarks,

$$\begin{aligned} & Q^2 \frac{dxq^s(x,Q^2)}{dQ^2} \\ &= \frac{\alpha_s(Q^2)}{2\pi}[P_{qq} \otimes q^s + P_{qg} \otimes g] \\ &- \frac{\alpha_s^2(Q^2)}{4\pi R^2 Q^2} \int_x^{1/2} \frac{dy}{y} x P_{gg\to q}(x,y)[yg(y,Q^2)]^2 \\ &+ \frac{\alpha_s^2(Q^2)}{4\pi R^2 Q^2} \int_{x/2}^{x} \frac{dy}{y} x P_{gg\to q}(x,y)[yg(y,Q^2)]^2, (if\ x \le 1/2), \\ & Q^2 \frac{dxq^s(x,Q^2)}{dQ^2} \\ &= \frac{\alpha_s(Q^2)}{2\pi}[P_{qq} \otimes q^s + P_{qg} \otimes g] \\ &+ \frac{\alpha_s^2(Q^2)}{4\pi R^2 Q^2} \int_{x/2}^{1/2} \frac{dy}{y} x P_{gg\to q}(x,y)[yg(y,Q^2)]^2, (if\ 1/2 \le x \le 1), \end{aligned} \tag{9}$$

for the symmetric sea quarks, and

$$\begin{aligned} & Q^2 \frac{dxg(x,Q^2)}{dQ^2} \\ &= \frac{\alpha_s(Q^2)}{2\pi}[P_{gq} \otimes \Sigma + P_{gg} \otimes g] \\ &- \frac{\alpha_s^2(Q^2)}{4\pi R^2 Q^2} \int_x^{1/2} \frac{dy}{y} x P_{gg\to g}(x,y)[yg(y,Q^2)]^2 \\ &+ \frac{\alpha_s^2(Q^2)}{4\pi R^2 Q^2} \int_{x/2}^{x} \frac{dy}{y} x P_{gg\to g}(x,y)[yg(y,Q^2)]^2, (if\ x \le 1/2), \\ & Q^2 \frac{dxg(x,Q^2)}{dQ^2} \\ &= \frac{\alpha_s(Q^2)}{2\pi}[P_{gq} \otimes \Sigma + P_{gg} \otimes g] \\ &+ \frac{\alpha_s^2(Q^2)}{4\pi R^2 Q^2} \int_{x/2}^{1/2} \frac{dy}{y} x P_{gg\to g}(x,y)[yg(y,Q^2)]^2, (if\ 1/2 \le x \le 1), \end{aligned} \tag{10}$$

for the gluon, where the factor $1/(4\pi R^2)$ is from the normalizing of the two-parton distribution, and R is the correlation length of the two initial partons. The linear evolution terms are from standard DGLAP evolution and the recombination functions of the nonlinear terms are expressed as

$$P_{gg\to g}(x,y) = \frac{9}{64}\frac{(2y-x)(72y^4-48xy^3+140x^2y^2-116x^3y+29x^4)}{xy^5},$$
$$P_{gg\to q}(x,y) = P_{gg\to\overline{q}}(x,y) = \frac{1}{96}\frac{(2y-x)^2(18y^2-21xy+14x^2)}{y^5}. \quad (11)$$

Although a next-to-leading order (NLO) evolution is preferred, the LO evolution is the important first step for the determination of the initial parton distributions.

III. RESULTS

By the global fit to the experimental data, the initial nonperturbative parton distributions are obtained to be

$$xu^v(x,\mu^2) = 9.09x^{0.944}(1-x)^{2.38}(1-4.3\sqrt{x}+6.8x),$$
$$xd^v(x,\mu^2) = 0.765(1-x)^{1.1}xu_v,$$
$$x\overline{u}^{as}(x,\mu^2) = 294x^{2.62}(1-x)^{3.4}[(1-x)^{16.5}+0.00147], \quad (12)$$
$$x\overline{d}^{as}(x,\mu^2) = 42.5x^{1.97}(1-x)^{7.5}[(1-x)^{4.2}+10^{-5}],$$

which are shown in Fig. 1. The first moment of asymmetric down quark is $< d^{as} >_1 = 0.261$ with $< d^{as} >_1 - < u^{as} >_1 = 0.118$. The other two free parameters in Eqs. (8-10) are determined to be $R = 3.977\ \mathrm{GeV}^{-1}$, $\mu^2 = 0.064\ \mathrm{GeV}^2$ with $\Lambda_{QCD} = 0.204\ \mathrm{GeV}$.

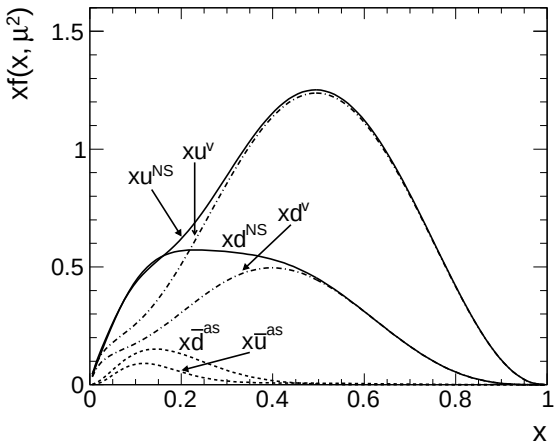

FIG. 1: The obtained initial parton distributions at $\mu^2 = 0.064\ \mathrm{GeV}^2$.

The x- and Q^2-dependence of the structure function $F_2^p(x,Q^2) = x\sum_i e_i^2 q_i^{NS}(x,Q^2) + x\sum_j e_j^2[q_j^s(x,Q^2)+\overline{q}_j^s(x,Q^2)]$ are shown in Figs. 2 and 3, respectively. The isoscalar structure functions xF_3 provide valuable informations of the valence quark distributions. Fig. 4 shows the predicted xF_3 with the experimental data. The ratios of the structure functions $F_2(x,Q^2)$ of the neutron to that of the proton are sensitive to up and down quark distributions. The calculated structure function ratios F_2^n/F_2^p under the assumption of the isospin symmetry between the proton and the neutron are shown in Fig. 5 with the experimental measurements. The predicted down to up valence quark ratios d^v/u^v are compared to the experimental data in Fig. 6. Basically, our predicted structure functions and valence quark distributions are consistent with the experimental measurements at high Q^2.

The obtained symmetric and asymmetric light sea quark distributions at different Q^2 are shown in Figs. 7 and 8, respectively. The predicted $\overline{d}-\overline{u} = \overline{d}^{as}-\overline{u}^{as}$ are shown in Fig. 9, compared to the E866 [4, 5] and HERMES [6] data, the CTEQ5M [33],

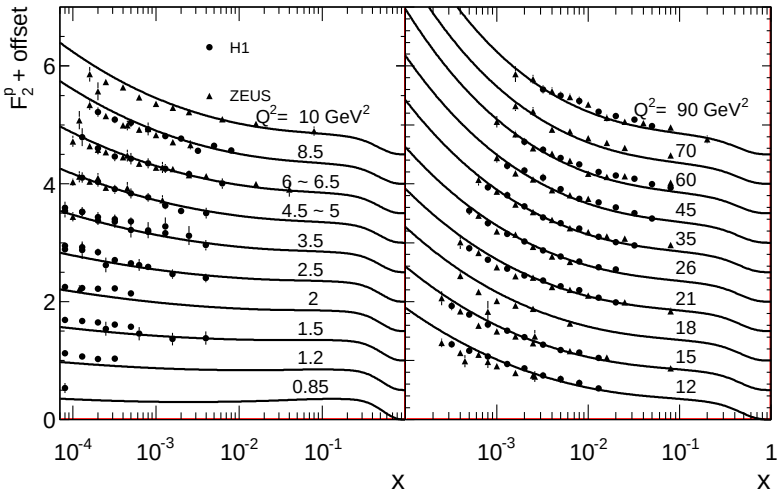

FIG. 2: Comparisons of the predicted x-dependence of F_2 to the experimental data from H1 [19] and ZEUS [20] at high Q^2.

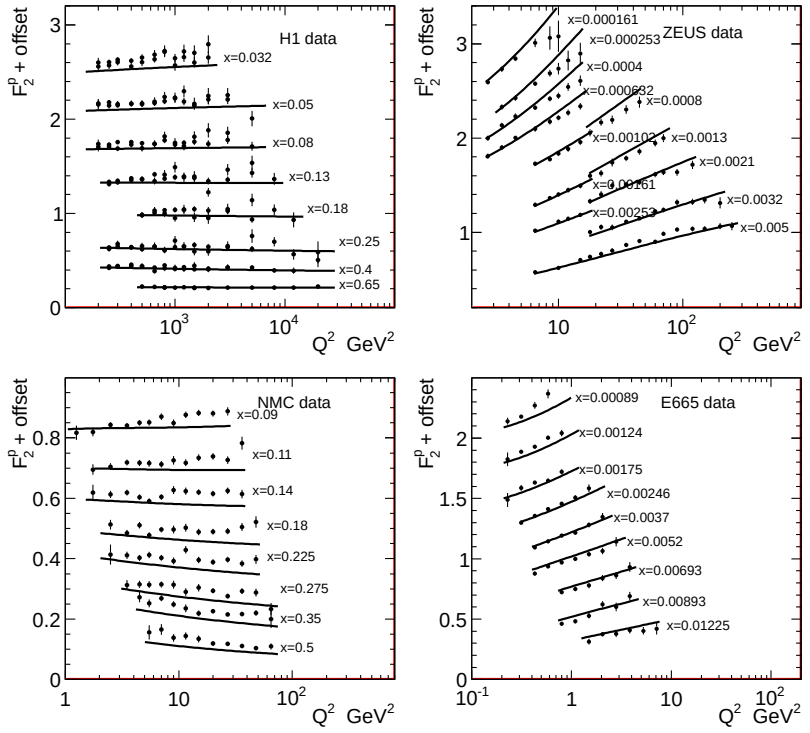

FIG. 3: Comparisons of the predicted Q^2-dependence of F_2 to the experimental data from H1 [21], ZEUS [22], NMC [23] and E665 [24] at large and small x.

GRV98 [9] and MSTW [34] parton distribution functions (Fig. 9(a)) and some models (Fig. 9(b)). The possible sign-change of $\overline{d}(x) - \overline{u}(x)$ around $x = 0.3$ is an interesting and important phenomenon for understanding the flavor structure of the nucleon sea [40]. Fig. 9(c) shows a very small negative value of $\overline{d} - \overline{u}$ in the range about $x > 0.3$, and the position where $\overline{d} - \overline{u} = 0$ is Q^2-dependent. The predicted ratios $\overline{d}/\overline{u}$ of the proton are shown in Fig. 10, compared to the E866 [4, 5] and NA51 [36] data, the global fits of CTEQ4M [7], CETQ5M [33], GRV98 [9] and MSTW [34] (Fig. 10(a)) and some models (Fig. 10(b)). Basically,

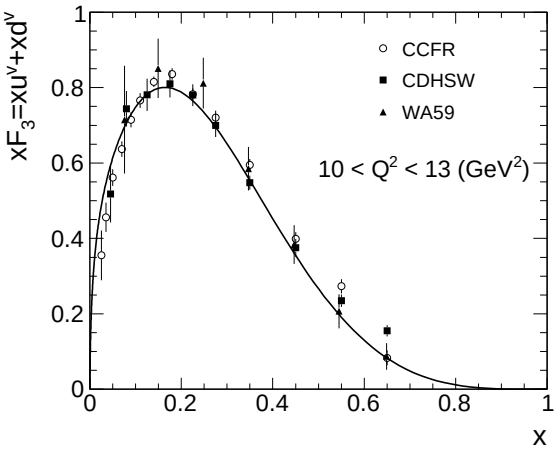

FIG. 4: Comparisons of the predicted xF_3 to the experimental data from CCFR [25], CDHSW [26] and WA59 [27].

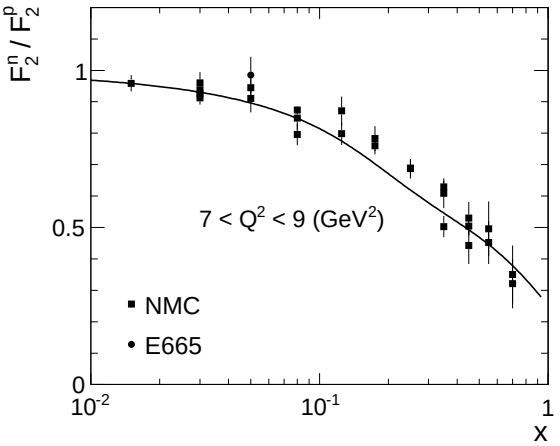

FIG. 5: Comparisons of the predicted structure function ratios F_2^n/F_2^p to the experimental data from NMC [28] and E665 [29].

the extracted symmetric and asymmetric light sea quark distributions are in agreement with the experimental measurements.

Strange quark describes some important features of the sea structure of the nucleon. However the relation between the strange sea and non-strange sea is rather confusing [41]. The decomposition of the asymmetric and symmetric sea in this work may provide a way to study the origin of the strange sea in the proton. As shown in Figs. 7 and 8, the asymmetric and symmetric sea have very different x- and Q^2-dependence. Assuming the $SU(3)_F$ flavor symmetry, we have $s + \overline{s} = \overline{u}^s + \overline{d}^s$. In this work, $s = \overline{s}$ is purely generated from the QCD evolution without any initial nonperturbative components, which is shown in Fig. 11 compared to the experiment. The experimental data is taken from the recent re-evaluation of the strange quark distribution of HERMES experiment [37]. Although the shape of our predicted strange quark distribution is similar to the HERMES data, the distribution is higher than the measurement. The breaking of the $SU(3)_F$ symmetry due to a large mass of the strange quark need to be considered. The popular PDFs from the CTEQ6L and GRV global fits are also shown in Fig. 11. For CTEQ6L strange quark distribution [38], the relation $s(x, Q_0^2) + \overline{s}(x, Q_0^2) = 0.4[\overline{u}(x, Q_0^2) + \overline{d}(x, Q_0^2)]$ is assumed at initial scale $Q_0^2 = 1.69$ GeV^2. The strange quark distribution in the GRV analysis [9] is also purely dynamically generated but starting from a high initial scale $Q_0^2 = 0.26\,\text{GeV}^2 \gg 0.064\,\text{GeV}^2$. The strange quark distribution in the GRV analysis is lower than the measurement at small x.

Usually the suppression ratio for strange quark $r_s = [s(x, Q^2) + \overline{s}(x, Q^2)]/2\overline{d}(x, Q^2) \neq 1$ is used to describe the $SU(3)_F$

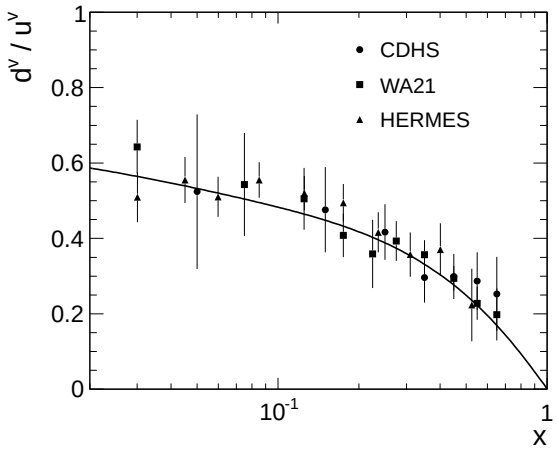

FIG. 6: Comparisons of the predicted valence quark ratios d^v/u^v to the measured data (Q^2 = 2.4 – 42.9 GeV^2) from CDHS [30], WA21 [31] and HERMES [32].

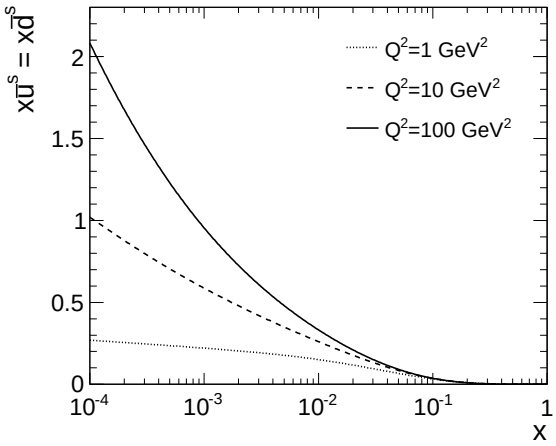

FIG. 7: The predicted symmetric light sea quark distributions in the proton at different resolution scales.

symmetry breaking. However, the ratio $\overline{d}(x)/\overline{u}(x)$ is strongly dependent on x due to the flavor-dependent asymmetric sea quark distributions $\overline{d}^{as}(x) \neq \overline{u}(x)^{as}$. We should exclude the contributions of $\overline{u}^{as}(x)$ and $\overline{d}(x)^{as}$ in the definition r_s. For this sake, we re-define the suppression ratio as

$$r_s(x, Q^2) = \frac{s(x, Q^2) + \overline{s}(x, Q^2)}{\overline{u}^s(x, Q^2) + \overline{d}^s(x, Q^2)}. \tag{13}$$

Strange quark distributions with different suppression values at Q^2 = 2.5 GeV^2 are shown in Fig. 12(a). It is found that the strange quark distribution with r_s = 0.8 is in excellent agreement with the HERMES measurement in $x < 0.07$ range. The preferred suppression ratio r_s = 0.8 is consistent with the ATLAS measurement [42] which obtains $r_s = 1.0 \pm 0.25$ at x = 0.023 and the lattice QCD calculation $r_s = 0.857 \pm 0.040$ at Q^2 = 2.5 GeV^2 [39]. However, the predicted strange quark distribution at large $x > 0.1$ is obviously higher than the experimental measurement. The suppression ratio is reduced to about 0.2 in large $x > 0.1$ region to meet the experiment. This may suggest an unknown mechanism for the strange quark production in the nucleon. Here, we list some phenomenological explanations: (1) the x-dependent suppression ratio $r_s(x)$, which is presented in Fig. 12(b); (2) the x-rescaling, i.e., $x[s(x, Q^2) + \overline{s}(x, Q^2)] = \eta x[\overline{u}^s(\eta x, Q^2) + \overline{d}^s(\eta x, Q^2)]$ at Q^2 = 2.5 GeV^2 with η = 0.8, which is

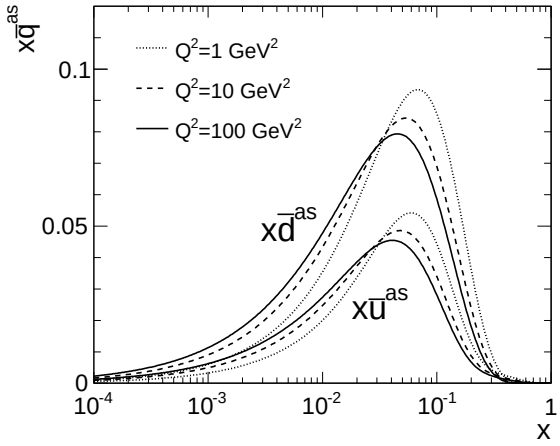

FIG. 8: The predicted asymmetric light sea quark distributions in the proton at different resolution scales.

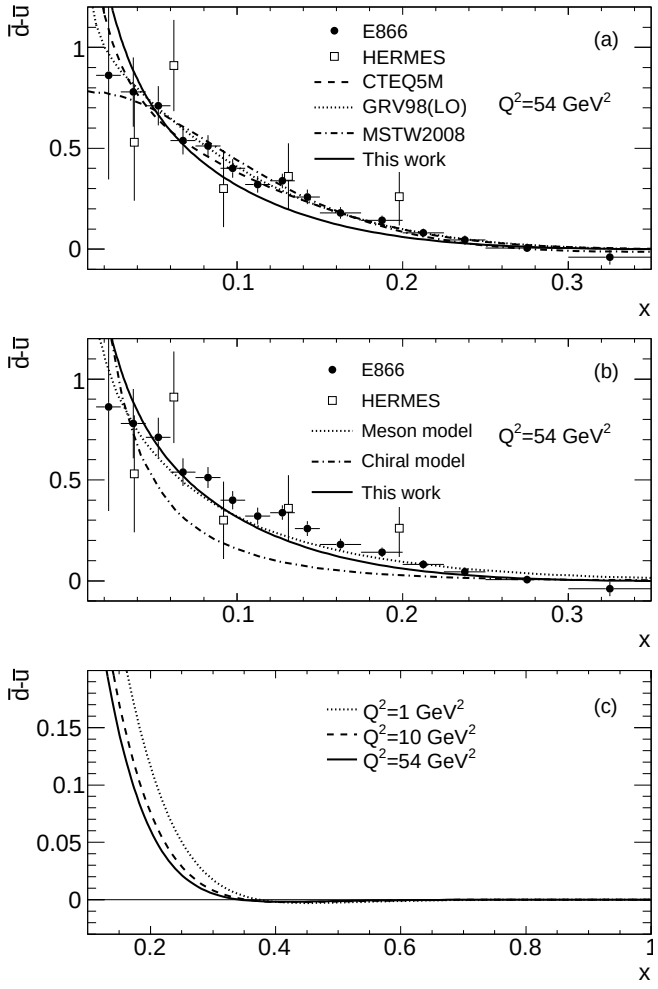

FIG. 9: Comparisons of the predicted light sea quark differences $\overline{d} - \overline{u}$ in the proton as a function of x at $Q^2 = 54$ GeV^2 to the experimental data from Fermilab E866 [4, 5] and HERMES [6]. (a) comparisons with the popular PDFs from CTEQ5M [33], GRV98 [9] and MSTW [34]; (b) comparisons with meson and chiral models [35]; (c) the possible sign-change of $\overline{d}(x) - \overline{d}(x)$ around $x = 0.3$ is shown.

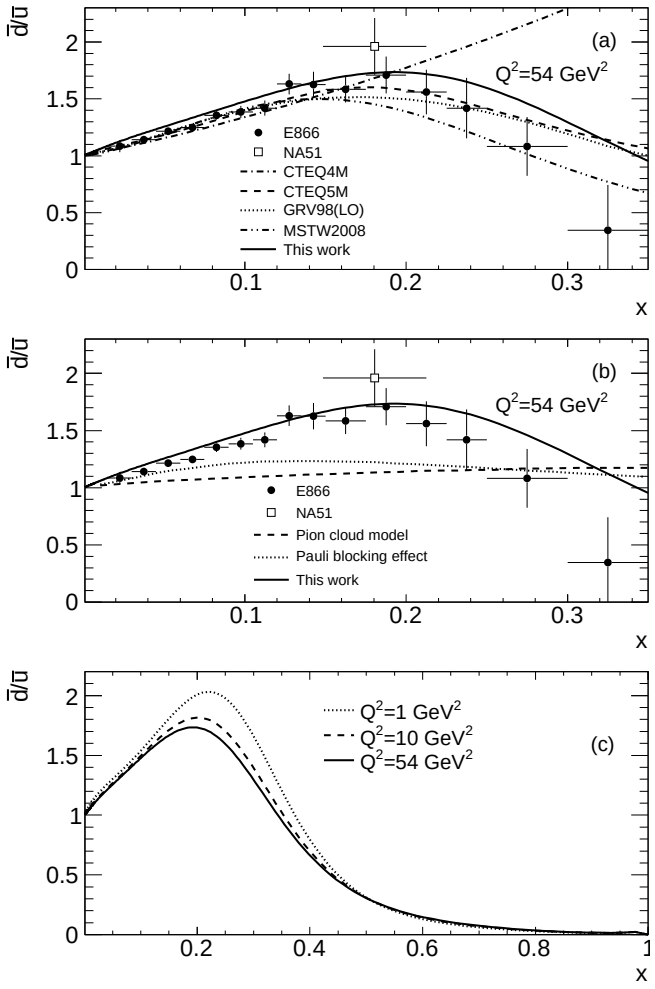

FIG. 10: Comparisons of the predicted light sea quark ratios $\overline{d}/\overline{u}$ in the proton as a function of x at $Q^2 = 54$ GeV^2 to the experimental data from Fermilab E866[4, 5] and NA51 [36]. (a) comparisons with the popular PDFs from CTEQ4M [7], CETQ5M [33], GRV98 [9] and MSTW [34]; (b) comparisons with meson model [35]; (c) the ratios $\overline{d}/\overline{u}$ at large x.

shown in Fig. 13; (3) the Q^2-rescaling, i.e., $x[s(x,Q^2)+\overline{s}(x,Q^2)] = x[\overline{u}^s(x,\zeta Q^2)+\overline{d}^s(x,\zeta Q^2)]$ with $\zeta = 0.2$ at $Q^2 = 2.5$ GeV^2, which is shown in Fig. 14.

In lattice QCD, the asymmetric light sea is related to the connected sea $u^{cs}(x)$ and $d^{cs}(x)$. The connected sea component has been determined by the calculation of lattice QCD, the previous HERMES result [43] and the CT10 parton distribution functions [44], which is given by

$$\begin{aligned}\overline{u}^{cs}(x,Q^2)+\overline{d}^{cs}(x,Q^2) &= [\overline{u}(x,Q^2)+\overline{d}(x,Q^2)]_{CT10} - \frac{1}{r_s^{lattice}}[s(x,Q^2)+\overline{s}(x,Q^2)]_{pre-HERMES} \\ &= \overline{u}^{cs}(x,Q^2)+\overline{d}^{cs}(x,Q^2)+\overline{u}^{ds}(x,Q^2)+\overline{d}^{ds}(x,Q^2) - \frac{1}{r_s^{lattice}}[s(x,Q^2)+\overline{s}(x,Q^2)]_{pre-HERMES},\end{aligned} \tag{14}$$

where the disconnected sea $\overline{u}^{ds}(x)$ and $\overline{d}^{ds}(x)$ are identical to our symmetric sea $\overline{u}^s(x)$ and $\overline{d}^s(x)$. Fig. 15 shows the comparison of our obtained asymmetric sea $x[\overline{u}^{as}(x,Q^2)+\overline{d}^{as}(x,Q^2)]$ with the connected sea $x[\overline{u}^{cs}(x,Q^2)+\overline{d}^{cs}(x,Q^2)]$ at $Q^2 = 2.5$ GeV^2. There are clear differences between the extracted asymmetric sea and the connected sea. The connected sea distribution is lower than the asymmetric sea distribution in the range about $x < 0.07$, while it is higher than the asymmetric sea distribution in the range about $x > 0.07$. The inconsistence is explained as follows. The strange quark distribution $s(x)+\overline{s}(x)$ for the determination of the connected sea is from the previous HERMERS data [43] which is higher than that from the current HERMES data [37] in the range of $x < 0.07$. As extracted by Eq. (14), the higher strange quark distribution results in the lower connected sea distribution

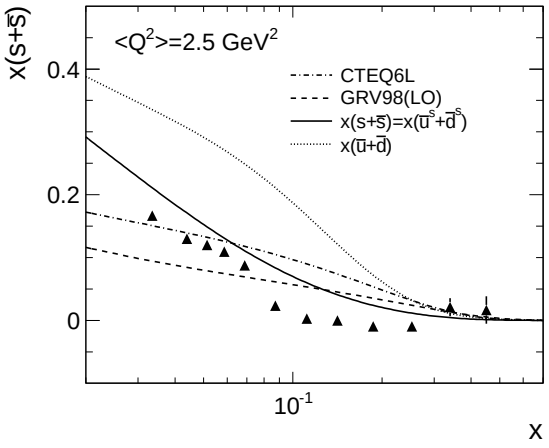

FIG. 11: Our predicted strange quark distribution $x[s(x,Q^2)+\overline{s}(x,Q^2)]$ at $Q^2 = 2.5$ GeV^2 compared to the HERMES data [37] and the global analyses from CTEQ6L [38] and GRV [9].

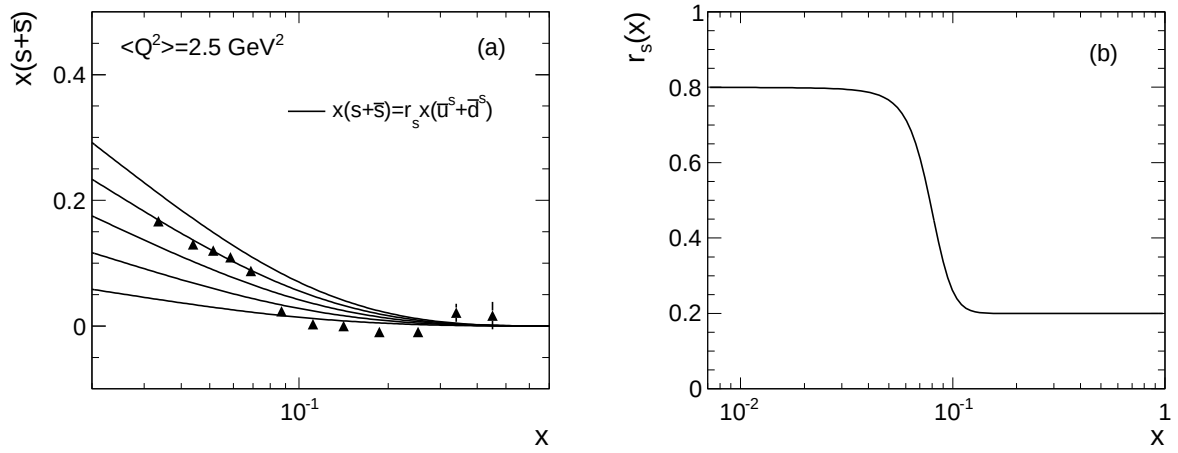

FIG. 12: (a) the strange quark distribution $x[s(x,Q^2)+\overline{s}(x,Q^2)]$ at $Q^2 = 2.5$ GeV^2 with different suppression values of $r_s = 1, 0.8, 0.6, 0.4$ and 0.2 (from top to bottom); (b) a possible curve of the suppression ratio $r_s(x,Q^2)$ as a function of x at $Q^2 = 2.5$ GeV^2.

in the small x region. In the lattice calculation [39], the disconnected sea is assumed to be $\overline{u}^{ds}(x) + \overline{d}^{ds}(x) = [s(x)+\overline{s}(x)]/r_s$ with r_s regarded as a constant. The fact is that the suppression ratio goes very small at large x. Hence the determined connected sea is higher than our extracted asymmetric sea at about $x > 0.07$. Generally, the obtained asymmetric light sea in this work is reasonable.

IV. DISCUSSIONS AND SUMMARY

The DGLAP equation with the parton recombination corrections at leading order is applied to the low Q^2 region. An unavoidable question is whether we can neglect all higher order QCD corrections when $Q^2 \ll 1$ GeV^2? Since all order resummation of these corrections are unable at moment, we suggest that if the leading order contributions (or including necessary lowest order corrections) are compatible with the experimental data, one may conjecture (1) these neglected higher order corrections may cancelable to each other; (2) or they are successfully absorbed by a finite number of free parameters such as μ^2 and R in

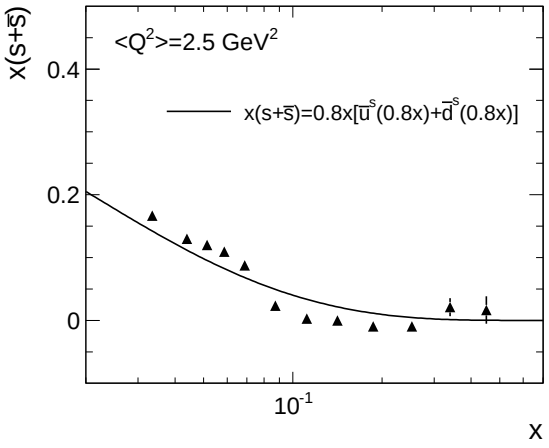

FIG. 13: The strange quark distribution $x[s(x,Q^2)+\bar{s}(x,Q^2)]$ at $Q^2 = 2.5$ GeV^2 by the x-rescaling model.

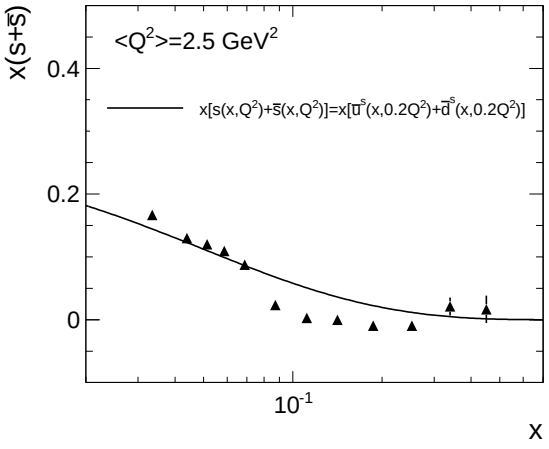

FIG. 14: The strange quark distribution $x[s(x,Q^2)+\bar{s}(x,Q^2)]$ at $Q^2 = 2.5$ GeV^2 by the Q^2-rescaling model.

this work. Before the confirmation of these conjectures, our initial parton distributions at $\mu^2 < 1$ GeV^2 can be regarded as an effective nonperturbative input which describe well the data at $Q^2 > 1$ GeV^2, as well as to predict the asymmetry light sea quark distributions in the proton.

In summary, the flavor asymmetric sea quark distributions in the proton are first extracted from the available experimental data by the DGLAP evolution with the parton recombination corrections. Moreover, with the separated flavor symmetric sea, we studied the possible relations between the strange quark distribution and the symmetric light quark distribution. It is found that the strange sea distribution is different from the non-strange distributions for that the former has few asymmetric nonperturbative components. Strange quark distributions from the x-dependent suppression ratio, the x-rescaling and the Q^2-rescaling models are basically consistent with the HERMES data. Finally, the extracted asymmetric sea component is in agreement with the connected sea in Lattice QCD if the re-evaluated data of the HERMES experiment is used and the x-dependent suppression ratio for the strange quark is assumed.

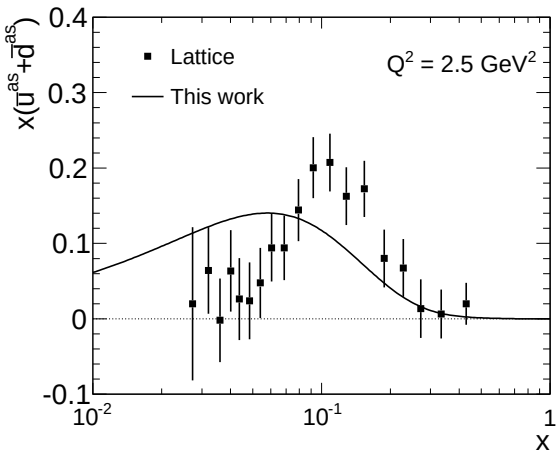

FIG. 15: Comparison of our predicted asymmetric light sea quark distribution $x[\overline{u}^{as}(x,Q^2)+\overline{d}^{as}(x,Q^2)]$ to the connected sea quark distribution $x[\overline{u}^{cs}(x,Q^2)+\overline{d}^{cs}(x,Q^2)]$ predicted by the lattice calculation [39] at $Q^2 = 2.5$ GeV^2.

Acknowledgments

One of us (W.Z.) thanks K.F. Liu for the useful discussions and suggestions.

Appendix: simplification of ZRS corrections to the DGLAP equation

The DGLAP equation with the complete ZRS corrections at leading order [15–17] according to Fig. 16 are written as

$$
\begin{aligned}
&Q^2\frac{dxq^{NS}(x,Q^2)}{dQ^2}\\
&=\frac{\alpha_s(Q^2)}{2\pi}P_{qq}\otimes q^{NS}\\
&-\frac{\alpha_s^2(Q^2)}{4\pi R^2Q^2}\int_x^{1/2}\frac{dy}{y}xP_{qg\to q}(x,y)yg(y,Q^2)yq^{NS}(y,Q^2)\\
&+\frac{\alpha_s^2(Q^2)}{4\pi R^2Q^2}\int_{x/2}^{x}\frac{dy}{y}xP_{qg\to q}(x,y)yg(y,Q^2)yq^{NS}(y,Q^2)\\
&-\frac{\alpha_s^2(Q^2)}{4\pi R^2Q^2}\int_x^{1/2}\frac{dy}{y}xP_{qq\to q}(x,y)y[\Sigma(y,Q^2)-q^{NS}(y,Q^2)]yq^{NS}(y,Q^2)\\
&+\frac{\alpha_s^2(Q^2)}{4\pi R^2Q^2}\int_{x/2}^{x}\frac{dy}{y}xP_{qq\to q}(x,y)y[\Sigma(y,Q^2)-q^{NS}(y,Q^2)]yq^{NS}(y,Q^2),(if\ x\le 1/2),\\
&Q^2\frac{dxq^{NS}(x,Q^2)}{dQ^2}\\
&=\frac{\alpha_s(Q^2)}{2\pi}P_{qq}\otimes q^{NS}\\
&+\frac{\alpha_s^2(Q^2)}{4\pi R^2Q^2}\int_{x/2}^{1/2}\frac{dy}{y}xP_{qg\to q}(x,y)yg(y,Q^2)yq^{NS}(y,Q^2)\\
&+\frac{\alpha_s^2(Q^2)}{4\pi R^2Q^2}\int_{x/2}^{1/2}\frac{dy}{y}xP_{qq\to q}(x,y)y[\Sigma(y,Q^2)-q^{NS}(y,Q^2)]yq^{NS}(y,Q^2),(if\ 1/2\le x\le 1),
\end{aligned}
\tag{15}
$$

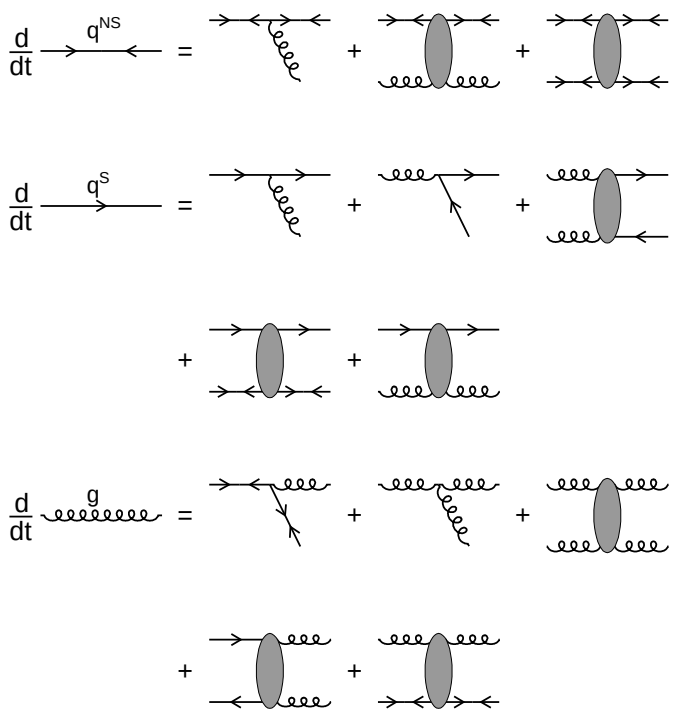

FIG. 16: Diagrams of the complete parton recombination corrections to the DGLAP evolution.

for the non-singlet quarks,

$$
\begin{aligned}
& Q^2 \frac{dxq^s(x,Q^2)}{dQ^2} \\
& = \frac{\alpha_s(Q^2)}{2\pi}[P_{qq} \otimes q^s + P_{qg} \otimes g] \\
& - \frac{\alpha_s^2(Q^2)}{4\pi R^2 Q^2} \int_x^{1/2} \frac{dy}{y} xP_{gg\to q}(x,y)[yg(y,Q^2)]^2 \\
& + \frac{\alpha_s^2(Q^2)}{4\pi R^2 Q^2} \int_{x/2}^{x} \frac{dy}{y} xP_{gg\to q}(x,y)[yg(y,Q^2)]^2 \\
& - \frac{\alpha_s^2(Q^2)}{4\pi R^2 Q^2} \int_x^{1/2} \frac{dy}{y} xP_{q\bar{q}\to q}(x,y)y\overline{q}^s(y,Q^2)yq^s(y,Q^2) \\
& + \frac{\alpha_s^2(Q^2)}{4\pi R^2 Q^2} \int_{x/2}^{x} \frac{dy}{y} xP_{q\bar{q}\to q}(x,y)y\overline{q}^s(y,Q^2)yq^s(y,Q^2) \\
& - \frac{\alpha_s^2(Q^2)}{4\pi R^2 Q^2} \int_x^{1/2} \frac{dy}{y} xP_{qq\to q}(x,y)y[\Sigma(y,Q^2) - q^s(y,Q^2)]yq^s(y,Q^2) \\
& + \frac{\alpha_s^2(Q^2)}{4\pi R^2 Q^2} \int_{x/2}^{x} \frac{dy}{y} xP_{qq\to q}(x,y)y[\Sigma(y,Q^2) - q^s(y,Q^2)]yq^s(y,Q^2) \\
& - \frac{\alpha_s^2(Q^2)}{4\pi R^2 Q^2} \int_x^{1/2} \frac{dy}{y} xP_{qg\to q}(x,y)yg(y,Q^2)yq^s(y,Q^2) \\
& + \frac{\alpha_s^2(Q^2)}{4\pi R^2 Q^2} \int_{x/2}^{x} \frac{dy}{y} xP_{qg\to q}(x,y)yg(y,Q^2)yq^s(y,Q^2), (if\ x \le 1/2), \\
& Q^2 \frac{dxq^s(x,Q^2)}{dQ^2} \\
& = \frac{\alpha_s(Q^2)}{2\pi}[P_{qq} \otimes q^s + P_{qg} \otimes g] \\
& + \frac{\alpha_s^2(Q^2)}{4\pi R^2 Q^2} \int_{x/2}^{1/2} \frac{dy}{y} xP_{gg\to q}(x,y)[yg(y,Q^2)]^2 \\
& + \frac{\alpha_s^2(Q^2)}{4\pi R^2 Q^2} \int_{x/2}^{1/2} \frac{dy}{y} xP_{q\bar{q}\to q}(x,y)y\overline{q}^s(y,Q^2)yq^s(y,Q^2) \\
& + \frac{\alpha_s^2(Q^2)}{4\pi R^2 Q^2} \int_{x/2}^{1/2} \frac{dy}{y} xP_{qq\to q}(x,y)y[\Sigma(y,Q^2) - q^s(y,Q^2)]yq^s(y,Q^2) \\
& + \frac{\alpha_s^2(Q^2)}{4\pi R^2 Q^2} \int_{x/2}^{1/2} \frac{dy}{y} xP_{qg\to q}(x,y)yg(y,Q^2)yq^s(y,Q^2), (if\ 1/2 \le x \le 1),
\end{aligned}
\tag{16}
$$

for the symmetric sea quarks and

$$
\begin{aligned}
&Q^2\frac{dxg(x,Q^2)}{dQ^2}\\
&=\frac{\alpha_s(Q^2)}{2\pi}[P_{gq}\otimes\Sigma+P_{gg}\otimes g]\\
&-\frac{\alpha_s^2(Q^2)}{4\pi R^2Q^2}\int_x^{1/2}\frac{dy}{y}xP_{gg\to g}(x,y)[yg(y,Q^2)]^2\\
&+\frac{\alpha_s^2(Q^2)}{4\pi R^2Q^2}\int_{x/2}^{x}\frac{dy}{y}xP_{gg\to g}(x,y)[yg(y,Q^2)]^2\\
&-\frac{\alpha_s^2(Q^2)}{4\pi R^2Q^2}\int_x^{1/2}\frac{dy}{y}xP_{q\overline{q}\to g}(x,y)\sum_q[yq^s(y,Q^2)]^2\\
&+\frac{\alpha_s^2(Q^2)}{4\pi R^2Q^2}\int_{x/2}^{x}\frac{dy}{y}xP_{q\overline{q}\to g}(x,y)\sum_q[yq^s(y,Q^2)]^2\\
&-\frac{\alpha_s^2(Q^2)}{4\pi R^2Q^2}\int_x^{1/2}\frac{dy}{y}xP_{qg\to g}(x,y)y\Sigma(y,Q^2)yg(y,Q^2)\\
&+\frac{\alpha_s^2(Q^2)}{4\pi R^2Q^2}\int_{x/2}^{x}\frac{dy}{y}xP_{qg\to g}(x,y)y\Sigma(y,Q^2)yg(y,Q^2),(if\ x\le 1/2),\\
&Q^2\frac{dxg(x,Q^2)}{dQ^2}\\
&=\frac{\alpha_s(Q^2)}{2\pi}[P_{gq}\otimes\Sigma+P_{gg}\otimes g]\\
&+\frac{\alpha_s^2(Q^2)}{4\pi R^2Q^2}\int_{x/2}^{1/2}\frac{dy}{y}xP_{gg\to g}(x,y)[yg(y,Q^2)]^2\\
&+\frac{\alpha_s^2(Q^2)}{4\pi R^2Q^2}\int_{x/2}^{1/2}\frac{dy}{y}xP_{q\overline{q}\to g}(x,y)\sum_q[yq^s(y,Q^2)]^2\\
&+\frac{\alpha_s^2(Q^2)}{4\pi R^2Q^2}\int_{x/2}^{1/2}\frac{dy}{y}xP_{qg\to g}(x,y)y\Sigma(y,Q^2)yg(y,Q^2),(if\ 1/2\le x\le 1),
\end{aligned}
\tag{17}
$$

for the gluons. The linear evolution terms are from the standard DGLAP evolution and the recombination functions $P_{ab\to c}$ are written as

$$
\begin{aligned}
P_{gg\to g}(x,y)&=\frac{9}{64}\frac{(2y-x)(72y^4-48xy^3+140x^2y^2-116x^3y+29x^4)}{xy^5},\\
P_{gg\to q}(x,y)&=P_{gg\to\overline{q}}(x,y)=\frac{1}{96}\frac{(2y-x)^2(18y^2-21xy+14x^2)}{y^5},\\
P_{qq\to q}(x,y)&=P_{\overline{q}\overline{q}\to\overline{q}}(x,y)=\frac{2}{9}\frac{(2y-x)^2}{y^3},\\
P_{q\overline{q}\to q}(x,y)&=P_{q\overline{q}\to\overline{q}}(x,y)=\frac{1}{108}\frac{(2y-x)^2(6y^2+xy+3x^2)}{y^5},\\
P_{qg\to q}(x,y)&=P_{\overline{q}g\to\overline{q}}(x,y)=\frac{1}{288}\frac{(2y-x)(140y^2-52yx+65x^2)}{y^4},\\
P_{qg\to g}(x,y)&=P_{\overline{q}g\to g}(x,y)=\frac{1}{288}\frac{(2y-x)^2(304y^2-202yx+79x^2)}{xy^4},\\
P_{q\overline{q}\to g}(x,y)&=\frac{4}{27}\frac{(2y-x)(18y^2-9yx+4x^2)}{xy^3}.
\end{aligned}
\tag{18}
$$

Our numerical calculations show that the following approximation is good, which is given by

$$
\begin{aligned}
&P_{qq\to q}(x,y) = P_{q\overline{q}\to\overline{q}}(x,y) = 0,\\
&P_{q\overline{q}\to q}(x,y) = P_{q\overline{q}\to\overline{q}}(x,y) = 0,\\
&P_{q\overline{q}\to g}(x,y) = 0,\\
&P_{qg\to q}(x,y) = P_{\overline{q}g\to\overline{q}}(x,y) = 0,\\
&P_{qg\to g}(x,y) = P_{\overline{q}g\to g}(x,y) = 0.
\end{aligned}
\tag{19}
$$

The reason is that the gluon density is significantly larger than the quark density at small x. Figure 17 shows the parton distribution functions at $Q^2 = 5$ GeV^2 using the complete recombination corrections (18) and the simplified recombination corrections (19) from the same initial parton distributions. The maximum relative deviation between these two evolutions is estimated to be smaller than 5%.

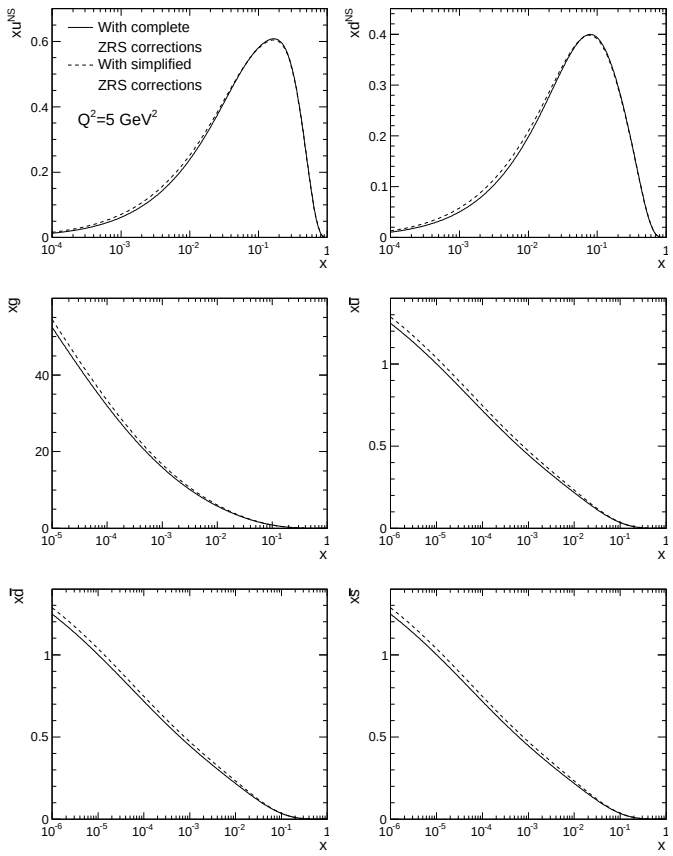

FIG. 17: Comparisons between the parton distribution functions from the complete ZRS corrections to the DGLAP evolution and that from the simplified ZRS corrections to the DGLAP evolution.

[1] K. Gottfried, Phys. Rev. Lett. **18**, 1174 (1967).

[2] P. Amaudruz et al. (New Muon Collaboration), Phys. Rev. Lett. **66**, 2712 (1991).

[3] M. Arneodo et al. (New Muon Collaboration), Phys. Rev. D **50**, R1 (1994).

[4] E. A. Hawker et al. (Fermilab E866/NuSea Collaboration), Phys. Rev. Lett. **80**, 3715 (1998).

[5] R. S. Towell et al. (FNAL E866/NuSea Collaboration), Phys. Rev. D **64**, 052002 (2001).

[6] K. Ackerstaff et al. (HERMES Collaboration), Phys. Rev. Lett. **81**, 5519 (1998).

[7] H. L. Lai et al., Phys. Rev. D **55**, 1280 (1997).
[8] A. D. Martin, R. G. Roberts, and W. J. Stirling, Phys. Lett. B **387**, 419 (1996).
[9] M. Glück, E. Reya, and A. Vogt, Eur. Phys. J. C **5**, 461 (1998).
[10] Y. L. Dokshitzer, Sov. Phys. JETP **46**, 641 (1977).
[11] V. N. Gribov, L. N. Lipatov, Sov. J. Nucl. Phys. **15**, 438 (1972).
[12] G. Altarelli, G. Parisi, Nucl. Phys. B **126**, 298 (1977).
[13] L. V. Gribov, E. M. Levin, and M. G. Ryskin, Phys. Rep. **100**, 1 (1983).
[14] A. H. Mueller and J. Qiu, Nucl. Phys. B **268**, 427 (1986).
[15] W. Zhu, Nucl. Phys. B **551**, 245 (1999) [arXiv:hep-ph/9809391].
[16] W. Zhu and J.H. Ruan, Nucl. Phys. B **559**, 378 (1999) [arXiv:hep-ph/9907330v2].
[17] W. Zhu and Z.Q. Shen, CPC (HEP & NP) **29**, 109 (2005) [arXiv:hep-ph/0406213v3].
[18] X.R. Chen, J.H. Ruan, R. Wang, P.M. Zhang and W. Zhu, Int. J. Mod. Phys. E **23**, 1450057 (2014).
[19] S. Aid et al. (H1 Collaboration), Nucl. Phys. B **470**, 3 (1996); C. Adloff et al. (H1 Collaboration), Nucl. Phys. B **497**, 3 (1997).
[20] M. Derrick et al. (ZEUS Collaboration), Z. Phys. C **69**, 607 (1996); M. Derrick et al. (ZEUS Collaboration), Z. Phys. C **72**, 399 (1996).
[21] C. Adloff et al. (H1 Collaboration), Eur. Phys. J. C **13**, 609 (2000) [hep-ex/9908059]; C. Adloff et al. (H1 Collaboration), Eur. Phys. J. C **19**, 269 (2001) [hep-ex/0012052]; C. Adloff et al. (H1 Collaboration), Eur. Phys. J. C **21**, 33 (2001) [hep-ex/0012053].
[22] S. Chekanov et al. (ZEUS Collaboration), Eur. Phys. J. C **21**, 443 (2001) [hep-ex/0105090].
[23] M. Arneodo et al. (New Muon Collaboration), Nucl. Phys. B **483**, 3 (1997) [hep-ph/9610231].
[24] M. R. Adams et al. (Fermilab E665 Collaboration), Phys. Rev. D **54**, 3006 (1996).
[25] W. G. Seligman et al. (CCFR Collaboration), Phys. Rev. Lett. **79**, 1213 (1997).
[26] P. Berge et al. (CDHSW Collaboration), Z. Phys. C **49**, 187 (1991).
[27] K. Varvell et al. (BEBC WA59 Collaboration), Z. Phys. C **36**, 1 (1987).
[28] D. Allasia et al. (New Muon Collaboration), Phys. Lett. B **249**, 366 (1990).
[29] M. R. Adams et al. (Fermilab E665 Collaboration), Phys. Rev. Lett. **75**, 1466 (1995).
[30] H. Abramowicz et al. (CDHS Collaboration), Z. Phys. C **25**, 29 (1984).
[31] G. T. Jones et al. (WA21 Collaboration), Z. Phys. C **62**, 601 (1994).
[32] J. E. Belz et al. (HERMES Collaboration), Proceedings of the 7th International Symposium on Meson-Nucleon Physics and the Structure of the Nucleon, Vancouver, Canada, 1997, edited by D. Drechsel, G. Hohler, W. Kluge, H. Leutwyler, H. M. Staudenmaier, and B. M. K. Nefkens (TRIUMF, Vancouver, Canada, 1997).
[33] H. L. Lai et al., Eur. Phys. J. C **12**, 375 (2000).
[34] A. D. Martin, W. J. Stirling, R. S. Thorne, and G. Watt, Eur. Phys. J. C **63**, 189 (2009).
[35] W. Melnitchouk, J. Speth and A. W. Thomas, Phys. Rev. D **59**, 014033 (1998).
[36] A. Baldit et al. (NA51 Collaboration), Phys. Lett. B **332**, 244 (1994).
[37] A. Airapetian et al. (HERMES Collaboration), Phys. Rev. D **89**, 097101 (2014) [arXiv:1312.7028v2].
[38] J. Pumplin et al., JHEP **07**, 012 (2002).
[39] Keh-Fei Liu, Wen-Chen Chang, Hai-Yang Cheng, and Jen-Chieh Peng, Phys. Rev. Lett. **109**, 252002 (2012).
[40] Jen-Chieh Peng et al., Phys. Lett. B **736**, 411 (2014) [arXiv:1401.1705v2].
[41] M. Stolarski, arXiv:1208.5427v3.
[42] G. Aad et al. (ATLAS Collaboration), Phys. Rev. Lett. **109**, 012001 (2012) [arXiv:1203.4051v2].
[43] A. Airapetian et al. (HERMES Collaboration), Phys. Lett. B **666**, 446 (2008) [arXiv:0803.2993v2].
[44] H. L. Lai, M. Guzzi, J. Huston, Z. Li, P. M. Nadolsky, J. Pumplin, and C.-P. Yuan, Phys. Rev. D **82**, 074024 (2010).